Cellular/Molecular

Reactive Oxygen Species Potentiate the $P2X_2$ Receptor Activity through Intracellular Cys^{430}

Claudio Coddou,[1,2] Juan F. Codocedo,[1] Shuo Li,[2] Juan G. Lillo,[1] Claudio Acuña-Castillo,[3] Paulina Bull,[1] Stanko S. Stojilkovic,[2] and J. Pablo Huidobro-Toro[1]

[1]Centro Regulación Celular y Patología Prof. J. V. Luco, Instituto Milenio de Biología Fundamental y Aplicada, Departamentos de Fisiología, Genética Molecular y Microbiología, Facultad de Ciencias Biológicas, Pontificia Universidad Católica de Chile, Santiago, Chile, [2]Section on Cellular Signaling, Program in Developmental Neuroscience, National Institute of Child Health and Human Development, National Institutes of Health, Bethesda, Maryland 20892, and [3]Departamento de Biología, Facultad de Química y Biología, Universidad de Santiago de Chile, Santiago, Chile

P2X receptor channels (P2XRs) are allosterically modulated by several compounds, mainly acting at the ectodomain of the receptor. Like copper, mercury, a metal that induces oxidative stress in cells, also stimulates the activity of $P2X_2R$ and inhibits the activity of $P2X_4R$. However, the mercury modulation is not related to the extracellular residues critical for copper modulation. To identify the site(s) for mercury action, we generated two chimeras using the full size $P2X_2$ subunit, termed $P2X_{2a}$, and a splice variant lacking a 69 residue segment in the C terminal, termed $P2X_{2b}$, as the donors for intracellular and transmembrane segments and the $P2X_4$ subunit as the donor for ectodomain segment of chimeras. The potentiating effect of mercury on ATP-induced current was preserved in *Xenopus* oocytes expressing $P2X_{4/2a}$ chimera but was absent in oocytes expressing $P2X_{4/2b}$ chimera. Site-directed mutagenesis experiments revealed that the Cys^{430} residue mediates effects of mercury on the $P2X_{2a}R$ activity. Because mercury could act as an oxidative stress inducer, we also tested whether hydrogen peroxide (H_2O_2) and mitochondrial stress inducers myxothiazol and rotenone mimicked mercury effects. These experiments, done in both oocytes and human embryonic kidney HEK293 cells, revealed that these compounds potentiated the ATP-evoked $P2X_{2a}R$ and $P2X_{4/2a}R$ currents but not $P2X_{2b}R$ and $P2X_{2a}$–C430A and $P2X_{2a}$–C430S mutant currents, whereas antioxidants dithiothreitrol and *N*-acetylcysteine prevented the H_2O_2 potentiation. Alkylation of Cys^{430} residue with methylmethane-thiosulfonate also abolished the mercury and H_2O_2 potentiation. Altogether, these results are consistent with the hypothesis that the Cys^{430} residue is an intracellular $P2X_{2a}R$ redox sensor.

Introduction

Reactive oxygen species (ROS) are chemically unstable, highly active molecules that include oxygen ions, free radicals, and peroxides. Although historically associated with pathological processes, including the cell damage by oxidative stress, there is considerable evidence indicating that ROS are also cell signaling molecules (Dröge, 2002). Within the past years, it has also become evident that the properties of ionic channels in the CNS and peripheral tissues are modified by ROS. Several voltage- and ligand-gated ionic channels are modulated by ROS, including voltage-gated channels (Chiamvimonvat et al., 1995; Annunziato et al., 2002), ryanodine receptor channels (Aracena-Parks et al., 2006), and purinergic P2X receptor channels (P2XRs) (Mason et al., 2004), strongly suggesting that ROS are acting or may act as modulators of neurotransmission.

Received May 4, 2009; revised June 26, 2009; accepted July 5, 2009.

This research was funded by Fondo de Investigación Avanzada en Áreas Prioritarias Grant 13980001 and by the Intramural Research Program of the National Institute of Child Health and Human Development/National Institutes of Health. The Millennium Institute for Fundamental and Applied Biology and Programa de Financiamento Basal Grant 12/2007 also contributed with funds.

Correspondence should be addressed to Dr. J. Pablo Huidobro-Toro, Departamento de Fisiología, Facultad de Ciencias Biológicas, Pontificia Universidad Católica de Chile, Alameda 340, Casilla 114-D, PC 6513677, Santiago, Chile. E-mail: jphuid@bio.puc.cl.

DOI:10.1523/JNEUROSCI.2096-09.2009

 0270-6474/09/2912284-08$15.00/0

Mercury is a heavy metal associated with cell damage; this metal has high affinity for sulfhydryl groups, inactivating enzymes, cysteine residues, and sulfur-containing antioxidants. Excess mercury results in a decrease of the antioxidant defense and a subsequent increase in oxidative stress (Annunziato et al., 2002); so mercury may act as an oxidative stress inducer (Nieminen et al., 1990; Lund et al., 1993). In the brain, mercury also causes behavioral and/or cognitive disturbances (Carpenter, 1994). This could reflect its action as an stress inducer but also as a direct modulator of ion channels, as indicated by its ability to interact with voltage- and ligand-gated ionic channels (Kiss and Osipenko, 1994). Mercury also affects the function of P2XRs, a family of two transmembrane domain ATP-gated channels (Surprenant and North, 2009). It potentiates the ATP-evoked currents in cells expressing $P2X_2R$ (Clyne et al., 2002; Lorca et al., 2005) and attenuates agonist-induced current in $P2X_4R$-expressing (Acuña-Castillo et al., 2000) and $P2X_7R$-expressing (our unpublished results) cells. Because modulation of P2XR activity induced by mercury shares the same pattern with copper, it was reasonable to hypothesize that both metals bind to a common allosteric site. However, this is not the case, as documented by Lorca et al. (2005) and Coddou et al. (2005).

Herein, we searched for a mercury binding site at the $P2X_{2a}R$ and ascertained whether ROS mimicked the action of this metal. Experiments were done with rat $P2X_2Rs$, $P2X_4R$, and their chi-

meras and mutants (see Fig. 1*A*), expressed in *Xenopus* oocytes and HEK293 cells. Both forms of $P2X_2$Rs, the full size receptor, termed $P2X_{2a}$R, and the shorter receptor form missing a 69 residue sequence in the C terminus, termed $P2X_{2b}$R (Koshimizu et al., 1998), as well as $P2X_4$R were used. We also used two chimeras that contain the ectodomain of the $P2X_4$ subunit and the transmembrane and cytoplasmic domains of $P2X_{2a}$ and $P2X_{2b}$ subunits (He et al., 2003). This strategy helped us to locate the residue that binds mercury in the C-terminal Val^{370}–Gnl^{438} sequence of the $P2X_{2a}$R. Using site-directed mutagenesis, we identified the Cys^{430} residue in this sequence as a putative target for the mercury-induced potentiation of the $P2X_{2a}$R. The same residue is also crucial for the potentiation induced by hydrogen peroxide (H_2O_2) and oxidative stress inducers, unmasking an intracellular redox sensor in this receptor.

Materials and Methods

Chemicals. ATP trisodium salt, H_2O_2, dithiothreitrol (DTT), *N*-acetylcysteine (NAC), myxothiazol, rotenone, and penicillin–streptomycin were purchased from Sigma-Aldrich. Mercury, copper, and zinc chlorides were obtained from Merck. Methylmethane-thiosulfonate (MMTS) was obtained from Toronto Research Chemical. The salts used to prepare the incubation media were purchased from Sigma-Aldrich or Merck. Samples of the triple-distilled water used in buffer preparation were analyzed for electroconductivity; trace metal contamination was assessed by inductively coupled plasma optical emission spectrometry using an Optima 2000 DV ICP-Emission Spectrometer (PerkinElmer Life and Analytical Sciences). Analysis revealed that trace metal contamination was <0.01 μM. ATP, metals, and H_2O_2 solutions were prepared daily before usage.

P2XRs used in experiments. All experiments were done with rat P2XRs (Fig. 1*A*). The difference between $P2X_{2a}$R and $P2X_{2b}$R splice forms is the lack of Val^{370}–Gln^{438} sequence in the C terminal in the later subunit (Koshimizu et al., 1998). The $P2X_{4/2a}$ and $P2X_{4/2b}$ chimeras contain the ectodomain of the $P2X_4$R (Ile^{66}–Tyr^{315}) instead of the $P2X_2$ subunit sequence (He et al., 2003). The $P2X_{2a}$–C430A and $P2X_{2a}$–C430S mutants were generated by PCR using the proofreading *Pfu* polymerase (Promega), followed by *Dpn*I digestion of the methylated parental plasmid. A 27-mer couple of primers were designed for the C430A mutant: sense, ggT gTC CAC ggA gCC Agg AgT gCA gTC ggC; antisense, Ctg TCC AgT CTC CTC ggC CTg CCT CCA TCT CTg C. For the C430S mutant, the following primers were designed: sense, gCT gTC CAg TCT CCT Cgg CCT AgC TCC ATC TCT gCT CTg ACT gA; antisense, TCA gTC AgA gCA gAg Atg gAg CTA ggC CgA ggA gAC Tgg ACA gC. To circumvent unwanted mutations, a region surrounding the targeted amino acid and presenting unique restriction sites was subcloned in the parental cDNA and then verified by automated sequencing.

Current measurements in oocytes. Experiments with *Xenopus* oocytes were conducted in accordance with the principles and procedures of the National Institutes of Health *Guide for the Care and Use of Laboratory Animals* and the Animal Ethical Committee of the P. Catholic University of Chile. A segment of the ovary was surgically removed under anesthesia from *Xenopus laevis* frogs; oocytes were manually defolliculated and incubated next with collagenase as detailed by Acuña-Castillo et al. (2000). Oocytes were injected intranuclearly with 3–5 ng of cDNA coding for the different rat receptors used. After a 36–48 h incubation in Barth's solution [in mM: 88 NaCl, 1 KCl, 2.4 $NaHCO_3$, 10 HEPES, 0.82 $MgSO_4$, 0.33 $Ca(NO_3)_2$, and 0.91 $CaCl_2$, pH 7.5] supplemented with 10 IU/L penicillin/10 mg streptomycin and 2 mM pyruvate, oocytes were clamped at −70 mV using the two-electrode voltage-clamp configuration with an OC-725C clamper (Warner Instruments). ATP-gated currents were recorded after regular 10 s ATP applications repeated every 10 min for up to 10 μM ATP; the percentage of change of the currents under these conditions was 1.2% in oocytes ($n = 217$), and in HEK293 cells, the percentage of current change was 1.3% ($n = 137$) under the same conditions. For higher ATP concentrations (>100 μM), the pulses were spaced up to 25 min to avoid receptor desensitization. After metal incubation, the recovery of control currents was always assessed. Noninjected oocytes did not evoke currents when exogenous ATP was applied. ATP, metal chloride salts, and amino acids were dissolved in Barth's media and perfused using a pump operating at a constant flow of 2 ml/min.

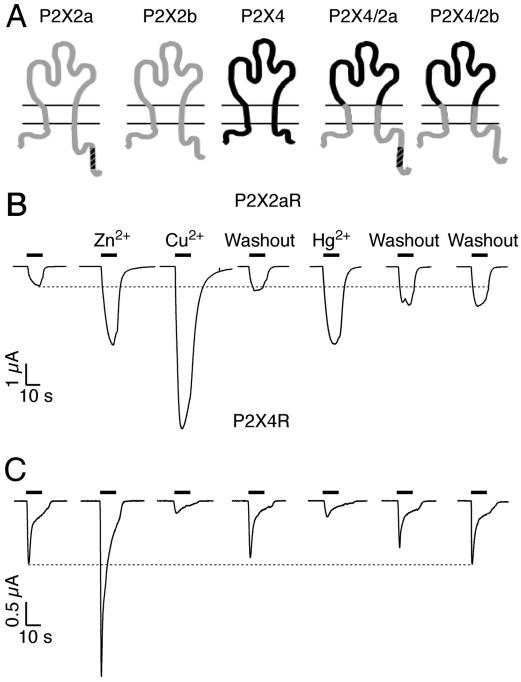

Figure 1. Parallelism in the actions of mercury and copper on $P2X_{2a}$R and $P2X_4$R activation. ***A***, Schematic representations of P2XRs used in this work. The $P2X_{4/2a}$ and $P2X_{4/2b}$ chimeras contain the extracellular Val^{66}–Tyr^{315} domain of the $P2X_4$ subunit (black) and the transmembrane and intracellular domains of the P2X2 subunits (gray); both splice forms of $P2X_2$ subunits, the full size $P2X_{2a}$ and the $P2X_{2b}$ subunit lacking the amino acid sequence Val^{370}–Gln^{438} in the C terminal, were used. ***B***, ***C***, Representative current traces from single oocytes expressing the homomeric $P2X_{2a}$R (***B***) and $P2X_4$R (***C***). ATP was repeatedly applied for 10 s (solid horizontal bars) at regular 10 min intervals in 30 μM (***B***) and 10 μM (***C***) concentrations. Each metal was preapplied in 10 μM concentrations for 1 min and coapplied with ATP. Horizontal dashed line represents the current response obtained with ATP alone, which served as control for these protocols. Notice that the effect of mercury on the peak amplitude of current was not completely reversible for the $P2X_{2a}$R after 10 and 20 min washouts.

Current measurements in HEK293 cells. HEK293 cells were routinely maintained in DMEM containing 10% (v/v) fetal bovine serum (Biofluids) and 100 μg/ml gentamicin (Invitrogen). Cells were plated on 25 mm poly-L-lysine (0.01% w/v; Sigma-Aldrich)-coated coverslips at a density of 1×10^5 cells per 35 mm dish. The transient transfection was conducted 24 h after plating the cells using 2 μg of DNA and 5 μl of LipofectAMINE 2000 reagent (Invitrogen) in 2 ml of serum-free Opti-MEM. After 4.5 h of incubation, the transfection mixture was replaced with normal culture medium. The experiments were performed 24–48 h after transfection. Electrophysiological experiments were performed on cells at room temperature using whole-cell patch-clamp recording techniques. The currents were recorded using an Axopatch 200B patch-clamp amplifier (Molecular Devices) and were filtered at 2 kHz using a low-pass Bessel filter. Patch electrodes, fabricated from borosilicate glass (type 1B150F-3; World Precision Instruments), using a Flaming Brown horizontal puller (P-87; Sutter Instruments), were heat polished to a final tip resistance of 2–4 MΩ. All current records were captured and stored using the pClamp 9 software packages in conjunction with the Digidata 1322A analog-to-digital converter (Molecular Devices). Patch electrodes were filled with a solution containing the following (in mM): 142 NaCl, 1 $MgCl_2$, 10 EGTA, and 10 HEPES, pH adjusted to 7.35 with 10 M NaOH. The osmolarity of the internal solutions was 306 mOsm. The bath solution contained the following (in mM): 142 NaCl, 3 KCl, 1 $MgCl_2$, 2 $CaCl_2$, 10 glucose, and 10 HEPES, pH adjusted to 7.35 with 10 M NaOH. The

osmolarity of this solution was 295–305 mOsm. ATP, H_2O_2, and metal solutions were daily prepared in bath buffer and applied using a fast gravity-driven microperfusion system (BPS-8; ALA Scientific Instruments). Stock solutions of the oxidative stress inductors were prepared in either ethanol or dimethylsulfoxide, and aliquots were stored at −20°C. The current responses were recorded from single cells clamped at −70 mV. Concentration–response data were collected from recordings of a range of ATP concentration applied to single cells with a washout interval of 5 min between each application and normalized to the highest current amplitude.

Data analysis. Concentration–response curves were performed applying ATP for 10 s in the 1–1000 μM dose range. Curves were normalized against the concentration of ATP that evoked the maximal response. For metal or H_2O_2 modulation experiments, at least five control ATP applications were performed; the average of all the control currents was used as the standard response (100%). The ATP median effective concentration (EC_{50}) was interpolated from each concentration–response curve. Likewise, the maximal ATP current (I_{max}) was obtained from each ATP concentration–response curve. Each protocol was performed in at least two separate batches of oocytes from different frogs; each experiment was repeated in at least four separate oocytes and HEK293 cells. Curve fitting was performed with GraphPad software. EC_{50}, IC_{50}, and I_{max} were obtained from each concentration–response curve. Receptor deactivation was expressed as the time between 10 and 90% decrease of the current amplitude after ATP removal, termed 10–90% deactivation time. Statistical analyses included Kruskal–Wallis and Mann–Whitney tests (GraphPad software), because we determined previously that nonparametric statistical tests are better fitted for our analysis as described (Acuña-Castillo et al., 2000).

Table 1. Characterization of P2XRs expressed in oocytes and HEK293 cells

Receptor	EC_{50} (μM)	n_H	I_{max}	n
Xenopus laevis oocytes				
P2X$_{2a}$	33.3 ± 2.5	1.4 ± 0.1	12.1 ± 2.9	30
P2X$_{2b}$	59.2 ± 9.1	1.4 ± 0.3	15.6 ± 1.9	6
P2X$_{2a}$–C430A	293 ± 70*	1.2 ± 0.3	1.2 ± 0.5*	8
P2X$_{2a}$–C430S	45.0 ± 6.3	1.4 ± 0.3	11.8 ± 0.8	4
P2X$_{4/2a}$	4.8 ± 0.6	0.9 ± 0.2	6.7 ± 1.5	9
P2X$_{4/2b}$	4.6 ± 2.4	1.2 ± 0.1	14.0 ± 1.5	15
P2X$_4$	11.0 ± 2.6	1.4 ± 0.2	4.7 ± 0.6	12
HEK293 cells				
P2X$_{2a}$	10.2 ± 1.3	1.2 ± 0.2	4.6 ± 0.3	8
P2X$_{2b}$	7.6 ± 1.3	1.1 ± 0.3	4.2 ± 0.9	4
P2X$_{2a}$–C430S	18.1 ± 3.3	1.5 ± 0.6	5.4 ± 0.9	6

The EC_{50} and n_H values were derived from the Hill equation. The maximal current (I_{max}) values (in microamperes for *Xenopus* and nanoamperes for HEK cells) were obtained applying a saturating concentration of ATP. *$p < 0.01$, Kruskal–Wallis test compared with the P2X$_{2a}$R.

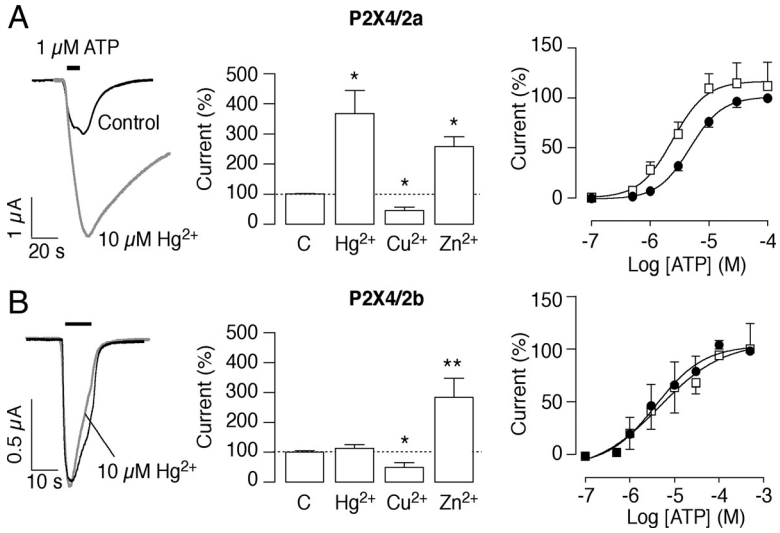

Figure 2. Effects of metal cations on P2X$_{4/2a}$ (***A***) and P2X$_{4/2b}$ (***B***) chimeras expressed in oocytes. Left column, The P2X$_{4/2a}$ chimera is mercury sensitive (top), whereas the P2X$_{4/2b}$ chimera is mercury resistant (bottom). Representative current traces from controls (black) and oocytes exposed to mercury 1 min before and during ATP application (gray). Middle column, Summary of effects of mercury, copper, and zinc, on the 1 μM ATP challenge; C refers to the control current in the absence of metals. Data shown are mean ± SEM values from four to six recordings per treatment; *$p < 0.05$, Kruskal–Wallis test. Right column, Concentration–response curves for ATP alone (filled circles) and ATP plus 10 μM mercury (open squares). The metal displaced leftward the nucleotide concentration–response curve for the P2X$_{4/2a}$ but not P2X$_{4/2b}$ chimera, reducing the ATP EC_{50} value from 4.8 ± 0.6 to 2.4 ± 0.6 μM ($p < 0.05$, Mann–Whitney test; $n = 5$–9 per dose). Mercury was preapplied for 1 min and then coapplied with ATP.

Results

Metal modulation of P2X$_{2a}$R and P2X$_4$R

Extracellularly applied zinc, copper, and mercury (all in 10 μM concentrations) potentiated the ATP-gated current in oocytes expressing P2X$_{2a}$R; representative traces are shown in Figure 1*B*. The potentiation of response by mercury was still present 20 min after the washout of metal (35 ± 12%) (Fig. 1*B*, last trace, $n = 6$), whereas a 10-min washout period was sufficient to restore normal response in oocytes treated with copper and zinc. In contrast to the P2X$_{2a}$R, mercury and copper inhibited ATP-induced P2X$_4$R currents; again, the effect of mercury was slower to reverse compared with copper or zinc, although it attained control currents within 20–30 min of washout (Fig. 1*C*, $n = 5$). Like in the P2X$_{2a}$R-expressing oocytes, zinc potentiated the responses evoked by ATP (Fig. 1*C*). In our experimental conditions, the ATP potency was threefold to fourfold higher for the P2X$_4$R than the P2X$_{2a}$R and P2X$_{2b}$R (Table 1) (supplemental Fig. 1, available at www. jneurosci.org as supplemental material). We also observed that mercury markedly influenced the rates of P2X$_{2a}$R deactivation, increasing the 10–90% deactivation time from 4.4 ± 0.2 to 17.2 ± 2.8 s ($n = 5$; $p < 0.05$) (supplemental Fig. 2, available at www.jneurosci.org as supplemental material). Such effect on the channel deactivation was also observed in the presence of copper, although the magnitude of the increase was only twofold (supplemental Fig. 2, available at www.jneurosci.org as supplemental material).

Potentiating effects of mercury in P2X$_{4/2a}$ but not P2X$_{4/2b}$ chimera-expressing oocytes

Because mercury has opposite effects on P2X$_2$R and P2X$_4$R activities, in additional studies, we used P2X$_{4/2}$ chimeras (Fig. 1*A*). The potentiating effect of mercury was preserved in P2X$_{4/2a}$-expressing cells, as indicated by the ability of 10 μM mercury to enhance the 1 μM ATP-induced current by 3.7 ± 0.8-fold (Fig. 2*A*). This potentiation reflected a leftward shift in the sensitivity of chimeras for ATP, reducing the EC_{50} from 4.8 ± 0.6 to 2.4 ± 0.6 μM ($n = 5$–9; $p < 0.05$) (Fig. 2*A*), without significantly altering the maximal ATP response. Zinc (10 μM) also potentiated the 1 μM ATP-evoked currents (2.6 ± 0.3-fold) (Fig. 2*A*), whereas 10 μM copper inhibited the ATP-evoked currents by 50% ($p < 0.05$) (Fig. 2*A*). In addition, copper did not significantly modify the ATP EC_{50} (3.3 ± 1.6 μM; $n = 5$), but it diminished the maximal ATP response by 40% (data not shown). Mercury also modified the receptor deactivation, as can be deduced from representative

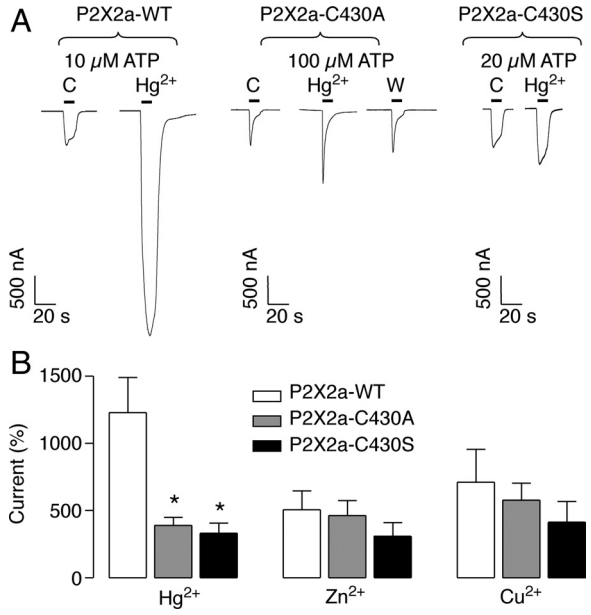

Figure 3. The mercury potentiation of ATP-induced current is significantly reduced in the C430 and C430S P2X$_2$R mutants expressed in oocytes. ***A***, Representative current responses to 10 s ATP applications (horizontal bars) using for each receptor an ATP approximate EC$_{15}$ concentration in controls (C), mercury-treated cells, and washout cells (W). Mercury was applied in 10 μM concentration 1 min before and during ATP application. ***B***, Comparison of the effects of metals on the peak amplitude of the ATP-evoked currents. Data shown are mean ± SEM values; *$p < 0.05$ compared with the P2X$_{2a}$R, Kruskal–Wallis test; $n = 4–6$. WT, Wild type.

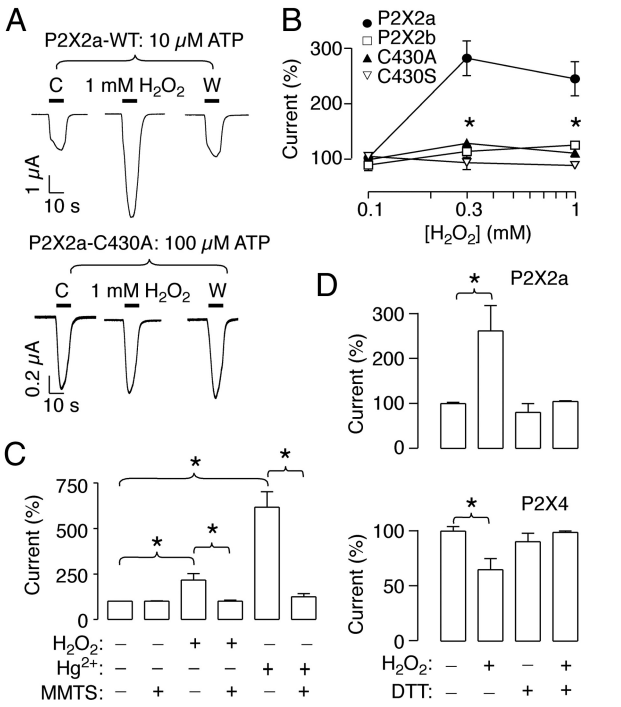

Figure 4. H_2O_2 potentiates the ATP-gated currents in the P2X$_{2a}$R expressed in oocytes in a Cys^{430}-dependent manner. ***A***, Representative current responses of the P2X$_{2a}$R (top) and the C430A mutant (bottom). H_2O_2 (1 mM) was applied for 10 min before the ATP pulse. C, Control; W, washout; WT, wild type. ***B***, Concentration-dependent effects of H_2O_2 on ATP-induced current in oocytes expressing wild-type and mutant P2X$_2$Rs. ***C***, Effects of chemical modification of cysteine residues in the P2X$_{2a}$R by the membrane-permeable MMTS on H_2O_2 or mercury-dependent potentiation of ATP-induced currents. MMTS was applied for 3 min before ATP application. ***D***, Summary of the effects elicited by H_2O_2, DTT, and the joint application of both agents on P2X$_{2a}$R (top) and P2X$_4$R (bottom) currents. In ***B–D***, ATP was applied in approximate EC$_{15}$ concentration for 10 s, and data shown are mean ± SEM values. *$p < 0.05$, Kruskal–Wallis test; $n = 4–6$ per dose/treatment.

tracings shown in Figure 2*A*; the 10–90% deactivation time augmented ninefold in the presence of mercury, from 12.6 ± 1.1 to 104.7 ± 11.5 s ($n = 5$; $p < 0.01$) (supplemental Fig. 2, available at www.jneurosci.org as supplemental material). Copper and zinc did not modify significantly the deactivation constant for this chimera (supplemental Fig. 2, available at www.jneurosci.org as supplemental material).

The P2X$_{4/2b}$ chimera was resistant to mercury (Fig. 2*B*), and 10 μM of the metal did not displace the ATP concentration–response curve (Fig. 2*B*) nor modified receptor deactivation. In contrast, 10 μM zinc potentiated the receptor activity by 2.6 ± 0.3-fold, whereas 10 μM copper significantly inhibited ATP-evoked currents by 55 ± 12% (Fig. 2*B*). As with the P2X$_{4/2a}$ chimera, the copper and zinc pattern was consistent with the extracellular domain of the chimera corresponding to the P2X$_4$R phenotype. The ATP EC$_{50}$ was 4.6 ± 2.4 μM (Table 1). These results indicate that the mercury-sensitive residue is located in the Val^{370}–Gln^{438} sequence of P2X$_2$R; this sequence contains a single cysteine at position 430.

Role of the Cys^{430} residue in the mercury-induced P2X$_{2a}$ receptor potentiation

To ascertain the role of this residue in the P2X$_{2a}$R sensitivity to mercury, we generated the P2X$_{2a}$–C430A and P2X$_{2a}$–C430S mutants of this receptor. The ATP potency for the P2X$_{2a}$–C430A mutant was reduced 10-fold compared with the wild type, and the receptor desensitization was markedly increased (Fig. 3*A*, Table 1). In contrast, the ATP EC$_{50}$ for the P2X$_{2a}$–C430S mutant and the rate of receptor desensitization were comparable with the wild-type receptor (supplemental Fig. 1, available at www.jneurosci.org as supplemental material) (Table 1) ($n = 4$). In both mutants, the potentiating effect of 10 μM mercury was significantly reduced but not completely abolished. In oocytes expressing the P2X$_{2a}$–C430A mutant, 10 μM mercury potentiated the ATP-evoked currents only 3.3 ± 0.7-fold compared with 12.3 ± 2.6-fold in the wild-type P2X$_{2a}$R ($p < 0.05$; $n = 5–6$) (Fig. 3*A*,*B*), whereas zinc and copper potentiation was not significantly altered (Fig. 3*B*). The effect of mercury in this mutant was totally reversible in contrast to the wild-type receptor (compare tracings of Figs. 3*A*, 1*A*). In cells expressing the P2X$_{2a}$–C430S mutant, 10 μM mercury potentiated by 2.2 ± 0.9-fold the ATP-evoked currents ($n = 4$). As with the P2X$_{2a}$–C430A mutant, copper and zinc potentiation was not changed in this mutant (Fig. 3*B*). Mercury also slowed the rate of P2X$_{2a}$R and P2X$_{4/2a}$ chimera deactivation, whereas the rates of P2X$_{2b}$R and P2X$_{4/2b}$ chimera were not significantly affected (supplemental Fig. 2, available at www.jneurosci.org as supplemental material). Such effect of mercury probably reflects increased sensitivity of receptors to ATP, which in turn delays dissociation of ATP from its binding during washout periods.

Interaction of mercury with ectodomain P2X$_{2a}$R residues

In additional work, we analyzed the Cys^{430} residue-independent effects of mercury on potentiation of the ATP-evoked currents. Experiments with P2X$_{4/2a}$–C430A and P2X$_{4/2b}$ chimeras revealed their insensitivity to mercury, in contrast to P2X$_{2b}$, P2X$_{2a}$–C430A, P2X$_{2a}$–C430S, and P2X$_{4/2a}$ receptors that showed a residual mercury-dependent potentiation. These results, shown in supplemental Figure 3 (available at www.jneurosci.org as supplemental material), indicate that the extracellular domain of the

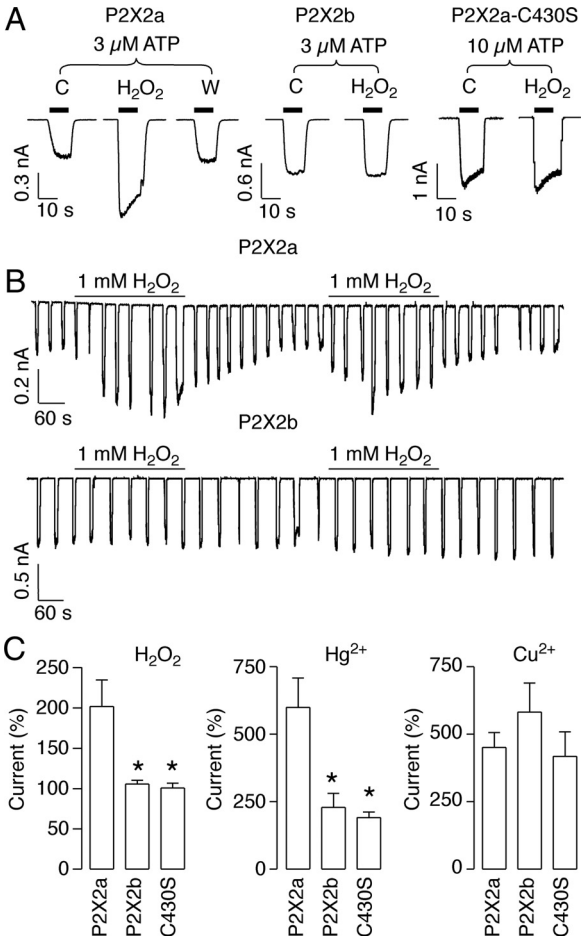

Figure 5. Potentiating effects of H_2O_2 on P2X$_{2a}$R but not P2X$_{2b}$R expressed in HEK293 cells. ***A***, Representative recordings from single cells expressing P2X$_{2a}$R, P2X$_{2b}$R, and P2X$_{2a}$–C430S mutant, showing the effect of 1 mM H_2O_2 on the ATP-evoked currents. Notice that H_2O_2 potentiation is observed only in cells expressing the P2X$_{2a}$R. C, Control; W, washout. ***B***, Effects of H_2O_2 on 3 μM ATP-stimulated current during repetitive agonist applications for 10 min in cells expressing P2X$_{2a}$R (top) and P2X$_{2b}$R (bottom). ***C***, Summary of the effects of H_2O_2, Hg^{2+}, and Cu^{2+} on ATP (approximate EC_{15} concentration) induced peak current in P2X$_{2a}$R, P2X$_{2b}$R, and P2X$_{2a}$–C430S mutant-expressing cells. Data shown are mean ± SEM values. *$p < 0.05$, Kruskal–Wallis test; $n = 4$–7 per group.

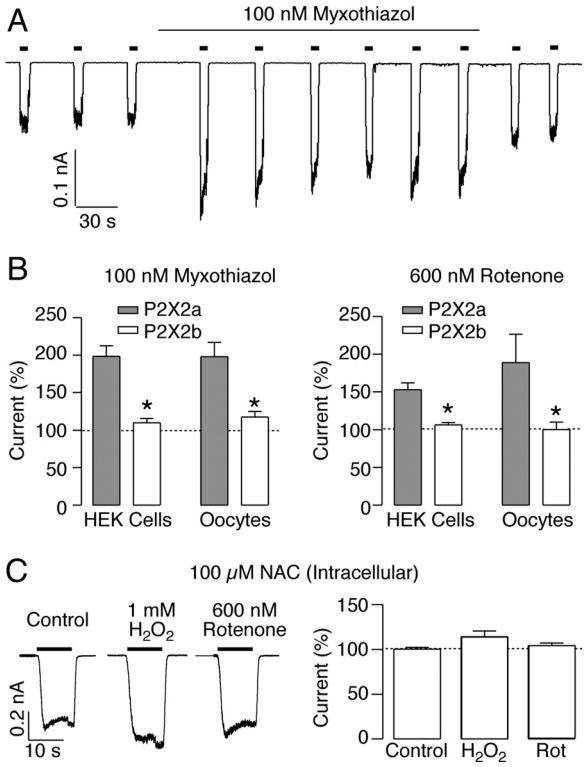

Figure 6. Effects of oxidative stress inducers on ATP-induced currents in P2X$_{2a}$R and P2X$_{2b}$R expressed in oocytes and HEK293 cells. ***A***, Representative recordings from a HEK293 cell expressing the P2X$_{2a}$R during repetitive application of 3 μM ATP in the presence and absence of 100 nM myxothiazol. ***B***, Summary of the effects of myxothiazol or 600 nM rotenone on the P2X$_{2a}$R (gray bars) and the P2X$_{2b}$R (white bars). In oocytes, these compounds were applied for 10 min before ATP application. Data shown are mean ± SEM values. *$p < 0.05$, Mann–Whitney test; $n = 4$–10. ***C***, NAC prevents H_2O_2 or rotenone (Rot)-dependent potentiation of 3 μM ATP-induced currents in HEK293 cells expressing the P2X$_{2a}$R; representative traces (left) and mean ± SEM values (right). $n = 4$–5.

P2X$_2$R contains additional residues that detect mercury directly or indirectly.

Effects of hydrogen peroxide on P2X$_2$R activity

The ATP-evoked P2X$_{2a}$R currents were potentiated by H_2O_2 in a concentration-dependent manner (Fig. 4*A*,*B*); 0.3 mM H_2O_2 increased by 2.8 ± 0.3-fold the ATP-gated currents (Fig. 4*B*). The P2X$_{4/2a}$ chimera was also potentiated by 1 mM H_2O_2, reaching a significant 1.9 ± 0.2-fold increase of the currents ($n = 4$). After 10 min washout, the currents remained increased 0.3 ± 0.1-fold. In contrast, P2X$_{2b}$R, P2X$_{4/2b}$ chimera, and P2X$_{2a}$–C430A and P2X$_{2a}$–C430S mutants were totally resistant to H_2O_2 (Fig. 4*A*,*B*). These results indicate that H_2O_2 mimics the Cys^{430} residue-dependent effects of mercury but not the minor extracellular-dependent action of this metal.

To confirm the role of cysteines in the H_2O_2-induced potentiation of P2X$_{2a}$R current, we chemically modified receptor cysteines using a plasma membrane-permeable MMTS. This reagent has an extremely rapid reactivity with thiol groups to form alkylthiosulfonated cysteines under normal physiological conditions (Valentine and Paglia, 1981). Oocyte treatment with 1 mM MMTS abolished the H_2O_2 potentiation in the wild-type P2X$_{2a}$R challenged with 10 μM ATP (Fig. 4*C*). MMTS treatment also abolished the mercury-induced potentiation (Fig. 4*C*). MMTS alone elicited a transient and reversible 20% current increase, but this effect reversed after the first washout (data not shown).

Conversely, the application of 1 mM DTT did not modify the ATP-evoked currents (Fig. 4*D*). The coapplication of H_2O_2 and DTT abolished the effect of H_2O_2 (Fig. 4*D*). Contrary to the P2X$_{2a}$R, 1 mM H_2O_2 inhibited by 43.8 ± 0.1% ($n = 4$) the P2X$_4$R activity (Fig. 4*D*). DTT application did not modify the receptor activity, but, when this agent was coapplied with H_2O_2, the inhibition was completely obliterated (Fig. 4*D*).

Effects of H_2O_2 and divalent metals on wild-type and mutant P2X$_2$Rs expressed in HEK293 cells

To exclude the cell-specific response to H_2O_2 and metals, in additional experiments, we used HEK293 cells as an expression system. In cells expressing the P2X$_{2a}$R, 1 mM H_2O_2 increased by 1.9 ± 0.3-fold the ATP-evoked currents (Fig. 5*A*,*C*, $n = 4$). The H_2O_2 potentiation had a slow onset and washout, as can be shown in a representative 10 min recording (Fig. 5*B*). Additionally, 10 μM Hg^{2+} increased by 5.9 ± 1.3-fold the ATP evoked-currents, and 10 μM Cu^{2+} induced a 4.5 ± 0.5-fold increase of the currents (Fig. 5*C*, $n = 4$–5). In parallel to experiments with oocytes, the P2X$_{2b}$R and the P2X$_{2a}$–C430S mutant expressed in

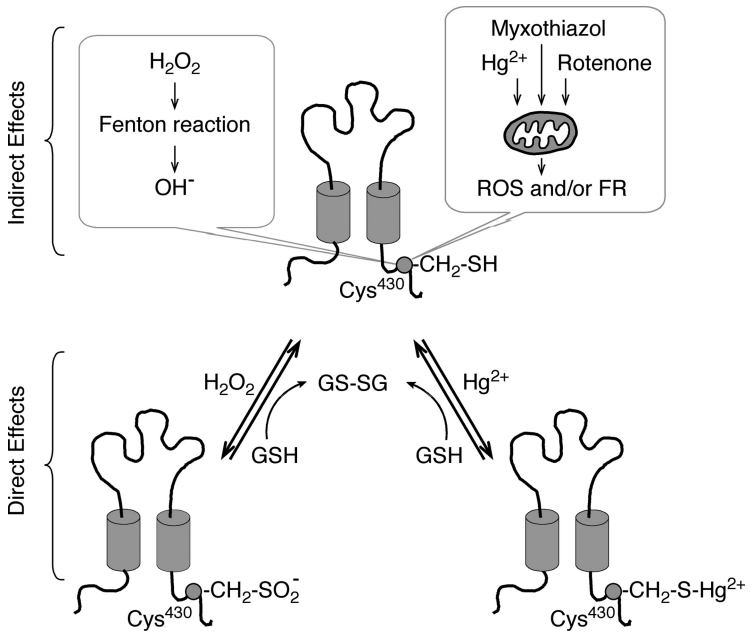

Figure 7. Possible mechanisms of P2X$_{2a}$R modulation by ROS, mercury, and stress inducers. The Cys^{430} residue could be oxidized by indirect and/or direct effects of H_2O_2 and mercury on receptors. Top, Indirect effects of H_2O_2, mercury and the oxidative stress inducers myxothiazol and rotenone could be mediated by ROS and free radicals (FR), including the hydroxyl radical OH^- produced by mitochondria. H_2O_2 could also generate OH^- through the Fenton reaction. Bottom, H_2O_2 or Hg^{2+} could also oxidize directly the SH group of the Cys^{430} residue; mercury forming a mercaptide product CH_2–S–Hg^{2+} and H_2O_2 inducing the oxidation of the thiol group to the corresponding sulfonic acid derivative CH_2–SO_2^-. The mercaptide could be rapidly formed because of the extreme affinity of mercury for thiols, whereas the sulfonic acid reaction might occur more slowly as a result of the formation of several intermediate reactive oxygen species that finally stabilize as the sulfonic acid derivative of Cys^{430}. Endogenous antioxidants such as glutathione (GSH) could partially revert these reactions, resulting in the reduction of the Cys^{430} residue and formation of glutathione/glutathione disulfide (GS-SG). The exogenous antioxidant DTT can mimic the action of glutathione (data not shown).

HEK293 cells were also completely resistant to H_2O_2 (Fig. 5*B*,*C*, $n = 4$–5). Mercury increased the ATP-gated currents in P2X$_{2b}$R and P2X$_{2a}$–C430S mutant by 2.5 ± 0.5- and 1.9 ± 0.2-fold, respectively, the values significantly lower to that obtained in the P2X$_{2a}$R ($p < 0.05$) (Fig. 5*C*, $n = 3$–5). Copper induced a 5.7 ± 1.5- and 4.2 ± 0.9-fold increase of the ATP-evoked currents in cells expressing P2X$_{2b}$R and P2X$_{2a}$–C430S mutant, respectively, values that do not differ from that obtained in the P2X$_{2a}$R, confirming the extracellular nature of the copper-induced potentiation (Fig. 5*C*, $n = 4$).

Effects of oxidative stress inducers

We next tested the effect of myxothiazol and rotenone, two oxidative stress inducers (Thierbach and Reichenbach, 1981; Dawson et al., 1993; Gonzalez-Flecha and Demple, 1995), on the P2X$_{2a}$R and P2X$_{2b}$R activity. In HEK293 cells expressing the P2X$_{2a}$R, 100 nM myxothiazol increased the ATP-evoked currents by 1.95 ± 0.14-fold (Fig. 6*A*,*B*, $n = 10$), a similar value to that observed in H_2O_2 treatment. Myxothiazol also potentiated the ATP-evoked currents in oocytes expressing the P2X$_{2a}$R, with a maximal potentiation of 1.95 ± 0.18-fold (Fig. 6*B*, $n = 5$). The effect of myxothiazol was biphasic; higher concentrations did not potentiate but rather inhibited the receptor activity (data not shown). In contrast, the P2X$_{2b}$R was insensitive to myxothiazol; the ATP-evoked currents were not affected by this agent when the receptor was expressed in both HEK293 cells and oocytes (Fig. 6*B*, $n = 3$–5). Rotenone also potentiated the activity of the P2X$_{2a}$R; 600 nM induced a 1.52 ± 0.08- and 1.75 ± 0.38-fold increase of the ATP-evoked currents in HEK293 cells and oocytes, respectively (Fig. 6*B*, $n = 5$–6). Again, this effect was not observed in HEK293 cells nor oocytes expressing the P2X$_{2b}$R (Fig. 6*B*, $n = 6$).

NAC prevents H_2O_2 and rotenone potentiation

We next tested the effect of NAC treatment on H_2O_2 or rotenone-induced potentiation. For this purpose, 100 μM NAC was added to the intracellular patch pipette solution. Under these conditions, neither 1 mM H_2O_2 nor 600 nM rotenone increased the ATP-evoked currents in HEK293 cells expressing the P2X$_{2a}$R (Fig. 6*C*).

Discussion

To understand the structural determinants of trace metal modulation in P2XR physiology, within the past years, we searched for critical residues linked to metal coordination in these receptors. The extracellular His^{120} and His^{213} are key residues for copper modulation in the P2X$_{2a}$R (Clyne et al., 2002; Lorca et al., 2005), whereas His^{140} and Asp^{138} are required for copper modulation in the P2X$_4$R (Coddou et al., 2003, 2007). However, the respective alanine mutants were all sensitive to mercury modulation, although they were completely copper resistant (Coddou et al., 2005; Lorca et al., 2005). These observations fostered the hypothesis that the site of mercury was different from that of copper in both the P2X$_{2a}$R and the P2X$_4$R. In this study, the use of the P2X$_{4/2}$ chimeras generated by He et al. (2003) was instrumental to identify the mercury site of action in the P2X$_{2a}$R. Comparing the sensitivity to trace metals and mercury in the P2X$_{4/2a}$ versus the P2X$_{4/2b}$ chimera, we deduced that the site of mercury was contained within the Val^{370}–Gln^{438} sequence of the P2X$_{4/2a}$ variant, located in the intracellular C terminal.

Based on the high chemical reactivity of sulfhydryl groups with mercury (Webb, 1966), we hypothesized that the Cys^{430} residue was critical for mercury and H_2O_2 modulation. Site-directed mutagenesis of this residue obliterated the mercury and H_2O_2-induced potentiation of the P2X$_{2a}$R activity. In addition, the uncharged and the plasma membrane-permeable thiol reagent MMTS (Valentine and Paglia, 1981) blunted both the effect of H_2O_2 and mercury, reinforcing the involvement of Cys^{430} in the modulation by these chemicals. H_2O_2 and mercury must be transported into the cell to reach their intracellular site of action. H_2O_2 crosses the oocyte cell membrane through aquaporins (Henzler and Steudle, 2000). In addition, an H_2O_2 gradient could be established across biological membranes, favoring its diffusion into the cell (Antunes and Cadenas, 2000; Seaver and Imlay, 2001). Mercury freely crosses the oocyte plasma membrane as a dichloride salt, an ionic species that rapidly diffuses the plasma membrane under our experimental conditions (Gutknecht, 1981). Mercury chloride has a high permeability rate because of its apolar nature and equilibrates with the oocyte cytoplasm within a few seconds (Webb, 1966; Huang and Narahashi, 1996).

According to our hypothesis, the oxidation state of Cys^{430} may vary depending on the availability of cell antioxidants, in-

cluding glutathione, ascorbic acid, β-carotene, and vitamin E, among others. Redox couples such as glutathione/glutathione disulfide and NADH/NAD^+ (nicotinamide adenine dinucleotide, reduced/nicotinamide adenine dinucleotide) will set the cell redox balance (Dröge, 2002); during a shift in the cell oxidation state, reflected in the likely oxidation of Cys^{430}, the P2XR function should increase. In this context, the results obtained with NAC are consistent with the involvement of endogenous glutathione/glutathione disulfide. NAC is a precursor of glutathione (Dröge, 2002), so its addition to cell cytoplasm will favor antioxidant mechanisms and consequently prevent ROS potentiation of $P2X_{2a}R$ activity. Consequently, in the presence of oxidative stress inducers myxothiazol or rotenone, we consistently observed an increase in the $P2X_{2a}R$ activity. It is known that these compounds increase ROS production by interfering at mitochondrial complexes (Dawson et al., 1993; Gonzalez-Flecha and Demple, 1995; Starkov and Fiskum, 2001). Mercury can also raise ROS levels acting in the mitochondria (Nieminen et al., 1990). These indirect effects are the most likely mechanism of action of these agents and are summarized in Figure 7. H_2O_2 could also act indirectly, by the formation of the free radical OH^-, through the Fenton reaction.

Alternatively, mercury or H_2O_2 could directly oxidize the Cys^{430} residue, leading to the formation of a stable mercaptide or sulfonic acid derivative, a reaction that should be irreversible in the case of mercury. The mercury-induced potentiation of the ATP-evoked currents was slowly reversed after washout. Although the extent of recovery varied between individual cells, we consistently observed an ~70% decrease in the current amplitude despite prolonged washout of this metal. This finding could be an indication that both direct and indirect mechanisms of the Cys^{430} residue oxidation might occur. Conversely, endogenous antioxidant defenses, such as glutathione/glutathione disulfide, may reverse the status of the Cys^{430} residue to its reduced state. Receptor recycling and trafficking of new synthesized receptors might also contribute in part to the recovery of basal receptor activity. Mirzoian and Luetje (2002) also discussed that the effect of mercury chloride on nicotinic receptors reversed slowly, persisting for several minutes after washout. In addition, the effects of mercury are described as slowly reversible or, in other cases, irreversible in several ionic channels and receptors (Gallagher et al., 1995; Huang and Narahashi, 1996; Mirzoian and Luetje, 2002). Interestingly, the effect of mercury on the $P2X_{2a}$–C430A and $P2X_{2a}$–C430S mutants was easily reversible, in contrast to its long-lasting effect on the wild-type receptor.

Several reasons might be invoked for the potentiation of the $P2X_{2a}R$ activity by mercury and H_2O_2, but the most likely explanation is an increase in the receptor affinity for ATP, a notion derived from the fact that mercury shifted leftward the ATP concentration–response curve. The alkylthiosulfonation of the Cys^{430}–$P2X_{2a}R$ residue, in contrast to treatment with mercury or hydrogen peroxide, did not augment the channel activity. This could be explained because MMTS reaction does not lead to a charged Cys^{430} derivative and is not a redox reaction, like in the case of H_2O_2 or mercury (Fig. 7). Additionally, we observed a residual mercury potentiation that was independent of Cys^{430} as it can be deduced from Figures 3 and 5*C* and supplemental Figure 3 (available at www.jneurosci.org as supplemental material). This could reflect that mercury also binds to extracellular receptor residue(s) of the $P2X_{2a}R$. Additional work is required to identify this (or these) residue(s).

In contrast to our results, Mason et al. (2004) reported that $P2X_2R$-mediated currents were inhibited by H_2O_2 in HEK293 cells, with a median effective concentration close to 1 mM. Moreover, H_2O_2 mimicked the hypoxia-induced $P2X_2R$ attenuation, establishing a link between receptor activity and ROS production. This finding prompted us to extend work with oocytes using HEK293 cells as an expression system. These experiments excluded the possibility that host cells influence effects of ROS and mercury. Several other reasons might explain these differences. We never exceeded 1 mM H_2O_2 because larger concentrations resulted in cell damage and membrane dissolution. In experiments with both cell types, we always observed a recovery of the response, even in long-lasting protocols (Fig. 5). We can rule out nonspecific effects because 1 mM H_2O_2 potentiates the $P2X_{2a}R$ but not the $P2X_{2b}R$ activity. In the work of Mason et al. (2004), it was also observed a transient increase followed by sustained inhibition of the $P2X_2R$-mediated currents after application of myxothiazol and rotenone. It is most likely that this transient increase corresponds to the potentiation that we now report, whereas the subsequent inhibition could be related to the cell death. These stress inducers were initially thought to decrease ROS production, but there is growing evidence that these agents do not diminish but rather increase ROS generation (Starkov and Fiskum, 2001).

Besides the diverse effects of ROS on voltage- and ligand-gated ionic channels (see Introduction), it has been proposed that H_2O_2 plays a role as an endogenous signal in physiological and pathophysiological conditions. In vascular tissues, for example, H_2O_2 might be one of the endothelium-derived hyperpolarizing factor(s) (Shimokawa and Matoba, 2004) and could participate in the intracellular signaling of the angiotensin II receptors augmenting NADPH oxidase activity (Touyz and Schiffrin, 2001), both of them important in regulation of the vascular tone. Moreover, several reports indicate that transduction pathways associated with protein kinase C or the arachidonic acid cascade can also regulate ROS production (Severson and Hee-Cheong, 1989). In the brain, H_2O_2 has been linked to long-term potentiation through protein kinase C or extracellular signal-regulated kinase activity or inhibiting phosphatases in the consolidation phase of long-term potentiation (Knapp and Klann, 2002).

In summary, we identified the Cys^{430} residue located in the $P2X_{2a}R$ intracellular C terminal as a target for mercury and H_2O_2-induced potentiation of ATP-evoked currents. Because both agents decreased the $P2X_4R$ activity, it is unlikely that the potentiation effects observed are attributable to nonspecific chemical reactions with other thiol groups of adjacent proteins or membrane components. The identification of Cys^{430} as a redox site in the $P2X_{2a}R$ allowed us to hypothesize that this intracellular residue senses the cell redox state, setting a novel property for the P2XRs. The present findings will allow the identification of other members of the P2XR family that may also have a redox sensor, unraveling the implications of intracellular cysteine residues on receptor physiology. Altogether, these findings highlight that P2XRs are not only sensors of extracellular ATP and allosteric modulators but may also respond to intracellular stimuli that vary depending on the metabolic state of the cell.

References

Acuña-Castillo C, Morales B, Huidobro-Toro JP (2000) Zinc and copper modulate differentially the P2X4 receptor. J Neurochem 74:1529–1537.

Annunziato L, Pannaccione A, Cataldi M, Secondo A, Castaldo P, Di Renzo G, Taglialatela M (2002) Modulation of ion channels by reactive oxygen and nitrogen species: a pathophysiological role in brain aging? Neurobiol Aging 23:819–834.

Antunes F, Cadenas E (2000) Estimation of H_2O_2 gradients across biomembranes. FEBS Lett 475:121–126.

Aracena-Parks P, Goonasekera SA, Gilman CP, Dirksen RT, Hidalgo C, Hamilton SL (2006) Identification of cysteines involved in S-nitrosylation, S-glutathionylation, and oxidation to disulfides in ryanodine receptor type 1. J Biol Chem 281:40354–40368.

Carpenter DO (1994) The public health significance of metal neurotoxicity. Cell Mol Neurobiol 14:591–597.

Chiamvimonvat N, O'Rourke B, Kamp TJ, Kallen RG, Hofmann F, Flockerzi V, Marban E (1995) Functional consequences of sulfhydryl modification in the pore-forming subunits of cardiovascular Ca^{2+} and Na^{+} channels. Circ Res 76:325–334.

Clyne JD, LaPointe LD, Hume RI (2002) The role of histidine residues in modulation of the rat P2X(2) purinoceptor by zinc and pH. J Physiol 539:347–359.

Coddou C, Morales B, González J, Grauso M, Gordillo F, Bull P, Rassendren F, Huidobro-Toro JP (2003) Histidine 140 plays a key role in the inhibitory modulation of the P2X4 nucleotide receptor by copper but not zinc. J Biol Chem 278:36777–36785.

Coddou C, Lorca RA, Acuña-Castillo C, Grauso M, Rassendren F, Huidobro-Toro JP (2005) Heavy metals modulate the activity of the purinergic P2X4 receptor. Toxicol Appl Pharmacol 202:121–131.

Coddou C, Acuña-Castillo C, Bull P, Huidobro-Toro JP (2007) Dissecting the facilitator and inhibitor allosteric metal sites of the P2X4 receptor channel: critical roles of CYS132 for zinc potentiation and ASP138 for copper inhibition. J Biol Chem 282:36879–36886.

Dawson TL, Gores GJ, Nieminen AL, Herman B, Lemasters JJ (1993) Mitochondria as a source of reactive oxygen species during reductive stress in rat hepatocytes. Am J Physiol 264:C961–C967.

Dröge W (2002) Free radicals in the physiological control of cell function. Physiol Rev 82:47–95.

Gallagher JD, Noelle RJ, McCann FV (1995) Mercury suppression of a potassium current in human B lymphocytes. Cell Signal 7:31–38.

González-Flecha B, Demple B (1995) Metabolic sources of hydrogen peroxide in aerobically growing *Escherichia coli*. J Biol Chem 270:13681–13687.

Gutknecht J (1981) Inorganic mercury (Hg^{2+}) transport through lipid bilayer membranes. J Membr Biol 61:61–66.

He ML, Zemkova H, Stojilkovic SS (2003) Dependence of purinergic P2X receptor activity on ectodomain structure. J Biol Chem 278:10182–10188.

Henzler T, Steudle E (2000) Transport and metabolic degradation of hydrogen peroxide in *Chara corallina*: model calculations and measurements with the pressure probe suggest transport of H_2O_2 across water channels. J Exp Bot 51:2053–2066.

Huang CS, Narahashi T (1996) Mercury chloride modulation of the GABAA receptor-channel complex in rat dorsal root ganglion neurons. Toxicol Appl Pharmacol 140:508–520.

Kiss T, Osipenko ON (1994) Toxic effects of heavy metals on ionic channels. Pharmacol Rev 46:245–267.

Knapp LT, Klann E (2002) Role of reactive oxygen species in hippocampal long-term potentiation: contributory or inhibitory? J Neurosci Res 70:1–7.

Koshimizu T, Tomiæ M, Van Goor F, Stojilkovic SS (1998) Functional role of alternative splicing in pituitary P2X2 receptor-channel activation and desensitization. Mol Endocrinol 12:901–913.

Lorca RA, Coddou C, Gazitúa MC, Bull P, Arredondo C, Huidobro-Toro JP (2005) Extracellular histidine residues identify common structural determinants in the copper/zinc P2X2 receptor modulation. J Neurochem 95:499–512.

Lund BO, Miller DM, Woods JS (1993) Studies on Hg(II)-induced H2O2 formation and oxidative stress in vivo and in vitro in rat kidney mitochondria. Biochem Pharmacol 45:2017–2024.

Mason HS, Bourke S, Kemp PJ (2004) Selective modulation of ligand-gated P2X purinoceptor channels by acute hypoxia is mediated by reactive oxygen species. Mol Pharmacol 66:1525–1535.

Mirzoian A, Luetje CW (2002) Modulation of neuronal nicotinic acetylcholine receptors by mercury. J Pharmacol Exp Ther 302:560–567.

Nieminen AL, Gores GJ, Dawson TL, Herman B, Lemasters JJ (1990) Toxic injury from mercuric chloride in rat hepatocytes. J Biol Chem 265:2399–2408.

Seaver LC, Imlay JA (2001) Hydrogen peroxide fluxes and compartmentalization inside growing *Escherichia coli*. J Bacteriol 183:7182–7189.

Severson DL, Hee-Cheong M (1989) Diacylglycerol metabolism in isolated aortic smooth muscle cells. Am J Physiol 256:C11–C17.

Shimokawa H, Matoba T (2004) Hydrogen peroxide as an endothelium-derived hyperpolarizing factor. Pharmacol Res 49:543–549.

Starkov AA, Fiskum G (2001) Myxothiazol induces H_2O_2 production from mitochondrial respiratory chain. Biochem Biophys Res Commun 281:645–650.

Surprenant A, North RA (2009) Signaling at purinergic P2X receptors. Annu Rev Physiol 71:333–359.

Thierbach G, Reichenbach H (1981) Myxothiazol, a new inhibitor of the cytochrome b-c1 segment of th respiratory chain. Biochim Biophys Acta 638:282–289.

Touyz RM, Schiffrin EL (2001) Increased generation of superoxide by angiotensin II in smooth muscle cells from resistance arteries of hypertensive patients: role of phospholipase D-dependent NAD(P)H oxidase-sensitive pathways. J Hypertens 19:1245–1254.

Valentine WN, Paglia DE (1981) Effect of chemical modification of sulfhydryl groups of human erythrocyte enzymes. Am J Hematol 11:111–124.

Webb J (1966) Mercurials. In: Enzyme and metabolic inhibitors. New York: Academic.